Ultrasonics 55 (2015) 75–84

Contents lists available at ScienceDirect

Ultrasonics

journal homepage: www.elsevier.com/locate/ultras

Resonance frequency and mass identification of zeptogram-scale nanosensor based on the nonlocal beam theory

Xian-Fang Li [a,b,*], Guo-Jin Tang [c], Zhi-Bin Shen [c], Kang Yong Lee [b]

[a] School of Civil Engineering, Central South University, Changsha 410075, PR China
[b] State Key Laboratory of Structural Analysis for Industrial Equipment, Dalian University of Technology, Dalian 116024, PR China
[c] College of Aerospace Science and Engineering, National University of Defense Technology, Changsha 410073, PR China

ARTICLE INFO

Article history:
Received 23 March 2014
Received in revised form 28 July 2014
Accepted 3 August 2014
Available online 10 August 2014

Keywords:
Mass identification
Nonlocal elasticity
Carbon nanotube-based sensor
Resonance frequency
Frequency shift

ABSTRACT

Free vibration and mass detection of carbon nanotube-based sensors are studied in this paper. Since the mechanical properties of carbon nanotubes possess a size effect, the nonlocal beam model is used to characterize flexural vibration of nanosensors carrying a concentrated nanoparticle, where the size effect is reflected by a nonlocal parameter. For nanocantilever or bridged sensor, frequency equations are derived when a nanoparticle is carried at the free end or the middle, respectively. Exact resonance frequencies are numerically determined for clamped-free, simply-supported, and clamped–clamped resonators. Alternative approximations of fundamental frequency are given in closed form within the relative error less than 0.4%, 0.6%, and 1.4% for cantilever, simply-supported, and bridged sensors, respectively. Mass identification formulae are derived in terms of the frequency shift. Identified masses via the present approach coincide with those using the molecular mechanics approach and reach as low as 10^{-24} kg. The obtained results indicate that the nonlocal effect decreases the resonance frequency except for the fundamental frequency of nanocantilever sensor. These results are helpful to the design of micro/nanomechanical zeptogram-scale biosensor.

1. Introduction

The purpose of this work is to study the frequency shift of transverse vibration of nanoscale beams when carrying a nanoparticle and to provide a mass identification formula for biosensors. Although mass identification formulae based on the classical beam theory are well known and they are a basis of conventional sensors for detecting mass, do these conclusions or formulae suit for biosensors? How do modify them so that they are capable of applying to nanoscale sensors?

In recent years, with a development of micro/nanoelectromechanical system, micro/nanoscale mass/force sensors have been widely used. For example, due to adhesion of virus, bacteria, and molecules to nanocantilever biosensors [1], their mass can be identified by comparing the frequency shift before and after the addition of attached mass. In addition, AFM probes [2] can be used to detect force interaction between the AFM tip and the material surface based on the structural response of nanocantilevers. So far, one-dimensional beam-like structures at nanoscale level such as carbon nanotubes (CNTs) and nanowires have been used to fabricate nanomechanical resonators and biosensors [3–7]. Therefore, the analysis of frequency shift for nanocantilevers and bridged nanobeams carrying attached mass is of significance for design of nanoscale biosensors. The fundamental frequencies of cantilevered or bridged single-walled CNTs can reach the level of 10 GHz–1.5 THz depending on the nanotubes' diameter and length [8]. The frequencies up to THz are beneficial to design zeptogram-scale sensors [9]. Using the classical beam theory, the use of single-walled CNTs as biosensors has been examined and approximate fundamental frequency shift is derived to detect the mass of biological objects by Chowdhury et al. [10]. A FEM simulation for the resonance frequency for cantilever and bridged CNTs carrying a concentrated mass is performed [11]. Furthermore, Adhikari and Chowdhury compared the resonance frequencies based on the classical Euler–Bernoulli beam theory and the molecular mechanics approach [12]. Although the frequency shift formulae are known based on the classical beam theory without size effect, it does not capture features at nanoscale level and then the well-known formulae do not reflect the nature of nanoscale sensors because of size-dependent material properties.

The material properties such as Young's modulus of CNTs [13] or nanowires [14] exhibit a size effect [15]. In the case of consider-

* Corresponding author at: School of Civil Engineering, Central South University, Changsha 410075, PR China. Tel.: +86 731 8816 7070; fax: +86 731 8557 1736.
E-mail address: xfli@csu.edu.cn (X.-F. Li).

http://dx.doi.org/10.1016/j.ultras.2014.08.002
0041-624X/

ation of the size effect, the influence of an attached mass on the resonance frequency is significant for identification of ultrasensitive atom-resolution mass [16]. In this field, using nonlocal elasticity beam theory, Murmu and Adhikari studied longitudinal vibration of a CNT with attached buckyballs at tip [17]. Using the Rayleigh quotient method, an approximate fundamental frequency of a nanocantilever with a mass at the free end has been obtained in [18]. If considering the effect of shear deformation and rotary inertia of cross-sections, Shen and co-authors employed the nonlocal Timoshenko beam theory to calculate resonance frequencies of several kinds of vibrating beam-mass systems of interest [19–21]. Natsuki et al. [22] studied the effect of axial tensile loads on vibration of nanomechanical mass sensor. Souayeh and Kacem [23] analyzed large amplitude nonlinear vibrations of electrostatically actuated CNT-based mass sensors. Murmu and Adhikari [24] employed the nonlocal beam theory to analyze resonance of a nanocantilever biosensor. Elishakoff et al. [25] investigated the resonance frequencies based on the nonlocal beam theory incorporating with the surface effect. Although the relationship between an attached mass and resonance frequency has been dealt with, an explicit dependence of mass identification on the frequency shift needs be further developed when considering the size effect. To explore the suitability of single-walled CNTs as a zeptogram-scale mass detector device for many sensing applications, an extensive and deep research on the dependence of resonance frequencies upon attached mass for nanocantilevered and bridged sensors is necessary.

This paper has threefold objectives: (1) to derive exact equations for the resonance frequencies of nanoscale resonators; (2) to provide explicit expressions for calculating the fundamental frequencies; (3) to establish formulae for identifying attached mass. To achieve the above objectives, this paper is organized as follows. In Section 2, nanoscale mass-beam resonators such as cantilevered and bridged sensors are analyzed, where the nonlocal effect is included. Exact frequency equations and approximate fundamental frequencies are derived. Section 3 is devoted to the examination of the accuracy of approximate frequencies and presentation of the formulae for mass identification. Also, our results are compared with others. Finally, conclusions are drawn.

2. Frequency equations for mass-beam resonators

Consider a CNT-based sensor with an attached nanoparticle such as bacterium, virus, buckyball. The most frequently-encountered vibration mode for mass sensors is flexural mode since they have relatively low natural frequencies and are readily excited for cantilever sensors. Due to the radius of gyration of the cross-section of CNT-based sensors being around the order of nanometer, which is close to the same order of the internal characteristic length, the vibrating beam exhibits a size effect. Hooke's law is recognized as constitutive equations to describe stress–strain relations of linear elastic media, which states that the stress components at any point in an elastic medium depend only upon the strain components at the same position. Hooke's law cannot capture the size effect. The nonlocal theory of elasticity states that the stress components at a reference point depend upon not only the strain components at the same position but also on all other points of the body [26]. Researches indicate that the size effect can be interpreted by the nonlocal theory of elasticity [17–21,24,25,27,28]. In the present paper, we invoke the nonlocal beam theory to study the vibration of nonlocal mass-beam resonators and show the dependence of the frequency shift on the nonlocal parameter.

For simplicity we adopt the simplest Euler–Bernoulli beam theory incorporating with the nonlocal effect. According to this theory, shear deformation and rotary inertia are still negligible. Thus, the governing equation of free vibration of flexural mode of nanoscale beams satisfies the transverse-wave equation

$$c^2 r_g^2 \frac{\partial^4 w}{\partial x^4} + \frac{\partial^2 w}{\partial t^2} - (e_0 a)^2 \frac{\partial^4 w}{\partial x^2 \partial t^2} = 0, \quad 0 < x < L, \tag{1}$$

where c denotes wave speed ($c = \sqrt{E/\rho}$, E being Young's modulus and ρ being the mass density), r_g the radius of gyration of the cross-section ($r_g = \sqrt{I/A}$, I being the second moment of cross-sectional area and A being the cross-sectional area), e_0 the dimensionless nonlocal parameter, a the internal characteristic length, and L the length of the nanoscale beam.

2.1. Nanocantilever

With reference to Fig. 1a, when a bucky ball or a virus, etc., is attached to the free end of a nanosensor, the bucky ball or virus is modeled as a nanoparticle with mass at zeptogram scale ($1\text{zg} = 10^{-24}$ kg). Here the mass is only considered as a concentrated mass or point mass, whereas its rotary inertia is neglected. Thus for a nanocantilever sensor carrying a mass m at tip $x = L$, the boundary conditions can be stated as

$$w = 0, \quad \frac{\partial w}{\partial x} = 0, \quad x = 0, \tag{2}$$

$$c^2 r_g^2 \frac{\partial^2 w}{\partial x^2} - (e_0 a)^2 \frac{\partial^2 w}{\partial t^2} = 0, \quad c^2 r_g^2 \frac{\partial^3 w}{\partial x^3} - (e_0 a)^2 \frac{\partial^3 w}{\partial x \partial t^2} = \frac{m}{\rho A} \frac{\partial^2 w}{\partial t^2}, \quad x = L. \tag{3}$$

It is pointed out that the boundary conditions at the free end with a nanoparticle are different from those based on the local (classical) Euler–Bernoulli beam theory because the bending moment $M = EI\partial^2 w/\partial x^2 - \rho A(e_0 a)^2 \partial^2 w/\partial t^2$ [27] instead of the classical one $M = EI\partial^2 w/\partial x^2$.

The general solution of the transverse-wave equation can be expressed as

$$w = e^{i\omega t}\left(C_1 \cos\frac{\omega x}{v} + C_2 \sin\frac{\omega x}{v} + C_3 \cosh\frac{\omega x}{v} + C_4 \sinh\frac{\omega x}{v}\right), \tag{4}$$

where ω is the angular frequency, $C_j (j = 1, 2, 3, 4)$ are constants which do not vanish simultaneously, and

$$v = \sqrt{\omega c r_g}, \tag{5}$$

is the phase velocity. For convenience of analysis, we introduce the following dimensionless variables

$$\xi = \frac{x}{L}, \quad \lambda = \frac{e_0 a}{L}, \quad \beta = \frac{m}{\rho A L}, \quad \Omega = \frac{\omega^2 L^2}{v^2}, \tag{6}$$

and the above governing Eq. (1) may be rewritten as

$$W^{IV} - \Omega^2 (W - \lambda^2 W'') = 0, \quad 0 < \xi < 1, \tag{7}$$

subjected to the boundary conditions

$$W(0) = W'(0) = 0, \tag{8}$$

$$W''(1) + \lambda^2 \Omega^2 W(1) = 0, \quad W'''(1) + \lambda^2 \Omega^2 W'(1) = -\beta \Omega^2 W(1), \tag{9}$$

where $w(x, t) = W(\xi)e^{i\omega t}$ is specified, the prime denotes differentiation with respect to ξ, and the time factor has been suppressed.

2.1.1. Frequency equation

First we determine the frequency equation of a vibrating mass-nanocantilever system. Upon the frequency equation is obtained, the resonance frequency can be determined through solving this equation. To this end, solving Eq. (7) we get w in (4) or W by removing the time factor

$$W = C_1 \cos k_1 \xi + C_2 \sin k_1 \xi + C_3 \cosh k_2 \xi + C_4 \sinh k_2 \xi, \tag{10}$$

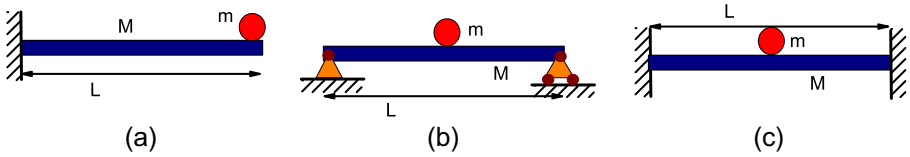

Fig. 1. Schematic of a flexural vibrating mass-beam system, (a) clamped-free beam with a tip mass; (b) simply-supported beam with mass at the middle; (c) clamped–clamped beam with mass at the middle.

where

$$k_1 = \sqrt{\frac{\sqrt{\lambda^4\Omega^4 + 4\Omega^2} + \lambda^2\Omega^2}{2}}, \quad k_2 = \sqrt{\frac{\sqrt{\lambda^4\Omega^4 + 4\Omega^2} - \lambda^2\Omega^2}{2}}. \tag{11}$$

Using the boundary conditions in (8), we get

$$C_1 + C_3 = 0, \tag{12}$$

$$C_2 k_1 + C_4 k_2 = 0. \tag{13}$$

Expressing C_3 and C_4 in terms of C_1 and C_2 and substituting them into (10), we have

$$W = C_1(\cos k_1\xi - \cosh k_2\xi) + C_2\left(\sin k_1\xi - \frac{k_1}{k_2}\sinh k_2\xi\right). \tag{14}$$

The first one of the boundary conditions in (9) allows us to eliminate C_1 or C_2 in (14). Application of the remaining one in (9) leads to the exact frequency equation of a vibrating mass-nanocantilever system

$$2 + \lambda^4\Omega^2 + 2\cos k_1\cosh k_2 + \lambda^2\Omega\sin k_1\sinh k_2 + \beta\sqrt{4 + \lambda^4\Omega^2}(k_1\cos k_1\sinh k_2 - k_2\sin k_1\cosh k_2) = 0, \tag{15}$$

where in the above derivation we have used the following relations

$$k_1^2 - k_2^2 = \lambda^2\Omega^2, \quad k_1^2 + k_2^2 = \Omega\sqrt{\lambda^4\Omega^2 + 4}, \quad k_1 k_2 = \Omega. \tag{16}$$

As a check, we set the dimensionless nonlocal parameter $\lambda = 0$, and then have $k_1 = k_2 = \sqrt{\Omega}$. Under such a circumstance, the frequency equation reduces to

$$1 + \cos\sqrt{\Omega}\cosh\sqrt{\Omega} + \beta\sqrt{\Omega}\left(\cos\sqrt{\Omega}\sinh\sqrt{\Omega} - \sin\sqrt{\Omega}\cosh\sqrt{\Omega}\right) = 0, \tag{17}$$

which is in consistency with that for a classical cantilever carrying a concentrated tip mass ([12,31], p. 214). Secondly, if attached mass vanishes, $\beta = 0$, we gain

$$2 + \lambda^4\Omega^2 + 2\cos k_1\cosh k_2 + \lambda^2\Omega\sin k_1\sinh k_2 = 0, \tag{18}$$

which is in exact agreement with that for free vibration of nonlocal cantilevers derived by Lu et al. [28].

2.1.2. Approximate fundamental frequency

Eq. (15) is a transcendental equation, and its solution, unfortunately, cannot be given in closed form, even for $\beta = \lambda = 0$, although its exact solution may be numerically determined with the aid of commercial software available. The transcendental Eq. (15) is still inconvenient for engineering application because of lack of an explicit expression for the dependence of the resonance frequency on the parameters β and λ.

In the following, an alternative integral equation is presented to derive an explicit closed-form expression for the resonance frequency of the fundamental vibration mode, which is the most significant in practice. To facilitate our analysis, let us introduce the curvature

$$\kappa(\xi) = \frac{d^2W}{d\xi^2}, \tag{19}$$

as a new unknown auxiliary function. Bearing this in mind, taking into account $W(0) = W'(0) = 0$ one obtains

$$W = \int_0^\xi (\xi - s)\kappa(s)ds. \tag{20}$$

Consequently, we substitute the above integral into (7) and then integrate both sides with respect to ξ twice, yielding

$$\kappa(\xi) - \frac{1}{6}\Omega^2\int_0^\xi (\xi - s)^3\kappa(s)ds + \Omega^2\lambda^2\int_0^\xi (\xi - s)\kappa(s)ds = (A\xi + B)\Omega^2, \tag{21}$$

where A and B are unknown constants, which can be determined using the conditions (9) at the free end. It is done by setting $\xi = 1$ in (21), i.e.

$$A = -\beta\int_0^1 (1 - s)\kappa(s)ds - \frac{1}{2}\int_0^1 (1 - s)^2\kappa(s)ds, \tag{22}$$

$$B = \beta\int_0^1 (1 - s)\kappa(s)ds + \frac{1}{2}\int_0^1 (1 - s)^2\kappa(s)ds - \frac{1}{6}\times\int_0^1 (1 - s)^3\kappa(s)ds. \tag{23}$$

Next, we plug these results back into (21) and find that $\kappa(\xi)$ must satisfy the following integral equation

$$\kappa(\xi) + \Omega^2\int_0^\xi K_1(\xi, s)\kappa(s)ds + \Omega^2\int_0^1 K_2(\xi, s)\kappa(s)ds = 0, \tag{24}$$

where

$$K_1(\xi, s) = (\xi - s)\left[\lambda^2 - \frac{1}{6}(\xi - s)^2\right], \tag{25}$$

$$K_2(\xi, s) = -(1 - s)\left[\beta(1 - \xi) + \frac{1}{2}(1 - \xi)(1 - s) - \frac{1}{6}(1 - s)^2\right]. \tag{26}$$

To obtain an explicit expression for the resonance frequencies, it is natural to assume that the curvature κ takes

$$\kappa(\xi) = \sum_{j=0}^{N} c_j\varphi_j(\xi), \tag{27}$$

where $\varphi_j(\xi)$'s are some base functions and N is a non-negative integer [29]. In what follows, we take $\varphi_j(\xi) = (1 - \xi)^{j+1}$. The first-order approximation of the fundamental frequency is obtained below

$$\Omega_1 = \frac{1}{\sqrt{\frac{11}{140} + \frac{1}{3}\beta - \frac{1}{10}\lambda^2}}. \tag{28}$$

If setting $\lambda = 0$, the above result is identical to that given in [10]. Furthermore, by comparing the above result with the exact one

$\Omega_1 = 3.516$ in the case of $\beta = \lambda = 0$, we find that a more accurate approximation may be taken as

$$\Omega_1 = \frac{1}{\sqrt{\frac{11}{136} + \frac{1}{3}\beta - \frac{1}{10}\lambda^2}} = \frac{3.516}{\sqrt{1 + 4.121\beta - 1.236\lambda^2}}. \tag{29}$$

In the absence of the nonlocal effect, $\Omega_1 = \sqrt{3/(\beta + 0.243)}$ follows from (29) and it has only a slight difference with the result $\Omega_1 = \sqrt{3/(\beta + 0.23)}$ ([30], p. 491). Nevertheless, it should be pointed out that the above approximation is different from the one derived by Murmu and Adhikari [24], who gave the following approximation according to the notations of the present paper

$$\Omega_1 = \frac{1}{\sqrt{\frac{11}{140} + \frac{1}{3}\beta + \frac{2}{5}\lambda^2}}. \tag{30}$$

By comparing (29) with (30), we find that a key discrepancy lies in the effect of the nonlocal parameter, which increases the resonance frequency if adopting (28) or (29), and decreases the resonance frequency if (30) is used. A comparison in detail of the above approximations with the exact resonance frequencies will be presented in the section of results and discussion.

Alternatively, if we choose $\varphi_j(\xi) = \cos(j\pi x/2)$, the first-order approximation is obtained to be

$$\Omega_1 = \frac{\pi^2}{2}\sqrt{\frac{\pi}{12\pi - 32 + 8\pi\beta - \lambda^2(4-\pi)\pi^2}}. \tag{31}$$

2.2. Simply supported nanobeams

For a simply-supported nanosensor carrying a nanoparticle, for simplicity we assume that an attached nanoparticle with mass m is at the middle, as shown in Fig. 1b. For this case, it is sufficient to solve the problem of the left half-beam part of the nanosensor. In other words, we solely determine the resonance frequencies of Eq. (1) subjected to the following boundary conditions

$$w = 0, \quad \frac{\partial^2 w}{\partial x^2} - \rho A (e_0 a)^2 \frac{\partial^2 w}{\partial t^2} = 0, \quad x = 0, \tag{32}$$

and

$$\frac{\partial w}{\partial x} = 0, \quad EI\frac{\partial^3 w}{\partial x^3} - \rho A (e_0 a)^2 \frac{\partial^3 w}{\partial x \partial t^2} = \frac{m}{2}\frac{\partial^2 w}{\partial t^2}, \quad x = \frac{L}{2}, \tag{33}$$

for symmetric modes, or

$$w = 0, \quad \frac{\partial^2 w}{\partial x^2} - \rho A (e_0 a)^2 \frac{\partial^2 w}{\partial t^2} = 0, \quad x = \frac{L}{2}, \tag{34}$$

for antisymmetric modes.

2.2.1. Frequency equation

It is clear that the boundary conditions (32) at end $x = 0$ correspond to vanishing deflection and bending moment, respectively. For those in (33), the first implies that the tangential at the middle of a simply-supported beam is horizontal, and the second implies the effect of the attached mass. After applying the boundary conditions (32) to a general solution (10), we find

$$W = C_2 \sin k_1\xi + C_4 \sinh k_2\xi. \tag{35}$$

Furthermore, making use of two conditions in (33) or (34) we can get the exact frequency equation

$$\frac{\beta\Omega}{2}\left(\frac{1}{k_1}\tan\frac{k_1}{2} - \frac{1}{k_2}\tanh\frac{k_2}{2}\right) = \sqrt{\lambda^4\Omega^2 + 4}, \tag{36}$$

for symmetric modes, or

$$\sin\frac{k_1}{2} = 0, \tag{37}$$

for antisymmetric modes. In this case an attached mass only affects the natural frequencies of vibration of symmetric modes, but does not affect those of antisymmetric modes. The reason is that the middle of a simply-supported beam where a nanoparticle is carried just coincides with the location of nodes of free vibration of antisymmetric modes.

Next, consider two special cases. One is the case of the absence of attached mass, meaning $\beta = 0$. From the above, one finds that the frequency Eq. (36) reduces to $\cos(k_1/2) = 0$, which together with $\sin(k_1/2) = 0$ gives $k_1 = n\pi$, identical to the result obtained in [28] through a different approach. Furthermore, one has

$$\Omega_n = \frac{n^2\pi^2}{\sqrt{1 + \lambda^2 n^2 \pi^2}}. \tag{38}$$

The dimensionless nonlocal parameter λ decreases the natural frequencies of a simply-supported nanobeam. The second special case is the case of no size effect, i.e. $\lambda = 0$. Thus from (36) it follows

$$\frac{4}{\beta} = \sqrt{\Omega}\left(\tan\frac{\sqrt{\Omega}}{2} - \tanh\frac{\sqrt{\Omega}}{2}\right). \tag{39}$$

This result is in consistency with the classical one ([31], p. 198), as expected.

2.2.2. Approximate fundamental frequency

Similar to the previous analysis, an approximate expression for the fundamental frequency can be obtained by using the integral equation method. We also denote the curvature $\kappa(\xi) = d^2W/d\xi^2$ as a new unknown function and have

$$W = \int_0^\xi (\xi - s)\kappa(s)ds + A\xi, \tag{40}$$

where A is an unknown constant. Consequently, substituting the above expression (40) into (7) yields

$$\kappa'' - \Omega^2\left(\int_0^\xi (\xi - s)\kappa(s)ds + A\xi - \lambda^2\kappa\right) = 0, \quad 0 < \xi < 1. \tag{41}$$

Integrating both sides of (41) with respect to ξ twice leads to

$$\kappa(\xi) - \frac{1}{6}\Omega^2\int_0^\xi (\xi - s)^3\kappa(s)ds + \Omega^2\lambda^2\int_0^\xi (\xi - s)\kappa(s)ds = \left(\frac{1}{6}A\xi^3 + B\xi + C\right)\Omega^2, \tag{42}$$

where B and C are also unknown constants to be determined. Since only symmetric vibration is focussed, using the first one in (33) one finds

$$A = -\int_0^{1/2} \kappa(s)ds. \tag{43}$$

Furthermore, from the second in (32) $C = 0$ can be deduced. Finally, making use of the second boundary condition in (33), we get

$$B = \frac{1}{2}\int_0^{1/2} s(1-s)\kappa(s)ds + \frac{\beta}{2}\int_0^{1/2} s\kappa(s)ds + \lambda^2\int_0^{1/2}\kappa(s)ds. \tag{44}$$

Next, we plug (43), (44) and $C = 0$ back into (42) and find that $\kappa(\xi)$ must satisfy the following integral equation

$$\kappa(\xi) + \Omega^2\int_0^\xi K_1(\xi, s)\kappa(s)ds + \Omega^2\int_0^{1/2} K_2(\xi, s)\kappa(s)ds = 0, \quad 0 \leqslant \xi \leqslant \frac{1}{2}, \tag{45}$$

where the kernel $K_1(\xi, s)$ is the same as that in (25) and

$$K_2(\xi, s) = -\xi\left[\frac{1}{2}s(1-s) - \frac{1}{6}\xi^2 + \lambda^2 + \frac{1}{2}\beta s\right]. \tag{46}$$

Similar to the treatment in the preceding subsection, if choosing $\varphi_j(\xi)=\sin(j\pi\xi)$, we obtain the first-order approximation of the fundamental frequency to be

$$\Omega_1=\frac{\pi^2}{\sqrt{1+2\beta+\pi^2\lambda^2}}. \tag{47}$$

It is clear that without any attached mass, (47) reduces to $\Omega_1=\pi^2/\sqrt{1+\pi^2\lambda^2}$, identical to the one given by (38) with $n=1$. A relation $\Omega_1=\pi^2/\sqrt{1+2\beta}$ is derived in the case of $\lambda=0$, which agrees well with $\Omega_1=\sqrt{48/(0.5+\beta)}$ ([30], p. 491).

2.3. Bridged nanobeams

Consider a clamped–clamped nanosensor or bridged nanobeam carrying a nanoparticle of mass m at the middle, as shown in Fig. 1c. For this case, it is still sufficient to solve the problem of the left half-beam part of the nanobeam due to symmetry. Thus we solely determine the resonance frequencies of Eq. (1) subjected to the following boundary conditions

$$w=0,\quad \frac{\partial w}{\partial x}=0,\quad x=0, \tag{48}$$

and

$$\frac{\partial w}{\partial x}=0,\quad EI\frac{\partial^3 w}{\partial x^3}-\rho A(e_0a)^2\frac{\partial^3 w}{\partial x\partial t^2}=\frac{m}{2}\frac{\partial^2 w}{\partial t^2},\quad x=\frac{L}{2}, \tag{49}$$

for symmetric mode, or

$$w=0,\quad \frac{\partial^2 w}{\partial x^2}-\rho A(e_0a)^2\frac{\partial^2 w}{\partial t^2}=0,\quad x=\frac{L}{2}, \tag{50}$$

for antisymmetric modes.

2.3.1. Frequency equation

In a similar manner we apply a general solution (10) in connection with the boundary conditions in (48) to get

$$W=C_1(\cos k_1\xi-\cosh k_2\xi)+C_2\left(\sin k_1\xi-\frac{k_1}{k_2}\sinh k_2\xi\right). \tag{51}$$

Furthermore, using two conditions in (49) or (50) one derives the frequency equation as follows

$$\cos\frac{k_1}{2}\left(\beta\Omega\cosh\frac{k_2}{2}+k_2\sqrt{\lambda^4\Omega^2+4}\sinh\frac{k_2}{2}\right)+\sin\frac{k_1}{2}\left(k_1\sqrt{\lambda^4\Omega^2+4}\cosh\frac{k_2}{2}+\frac{1}{2}\beta\lambda^2\Omega^2\sinh\frac{k_2}{2}\right)=\beta\Omega, \tag{52}$$

for symmetric modes, or

$$\frac{1}{k_1}\tan\frac{k_1}{2}-\frac{1}{k_2}\tanh\frac{k_2}{2}=0, \tag{53}$$

for antisymmetric modes. It is again seen that the natural frequencies of free vibration of the antisymmetric mode is free of the attached mass. This is because an attached mass just lies at the middle of a clamped–clamped nanobeam.

Next, we still consider two limiting cases. One is the case of the absence of attached mass, meaning $\beta=0$. In this case, one finds that the frequency Eq. (52) reduces to

$$k_1\tan\frac{k_1}{2}+k_2\tanh\frac{k_2}{2}=0. \tag{54}$$

It is worth noting that in [28], the frequency equation of a clamped–clamped nanobeam was derived to be

$$\lambda^2\Omega\sinh k_2\sin k_1+2\cosh k_2\sin k_1=2. \tag{55}$$

It is proven that our results are identical to that in [28] since Eq. (55) may be decomposed into Eqs. (54) and (53) for the symmetric and antisymmetric modes, respectively. The other limiting case is $\lambda=0$, meaning the case of classical clamped–clamped beams without the nonlocal effect. In this case, the results ([31], p. 208)

$$\sinh\frac{\sqrt{\Omega}}{2}\cos\frac{\sqrt{\Omega}}{2}+\cosh\frac{\sqrt{\Omega}}{2}\sin\frac{\sqrt{\Omega}}{2}=\frac{\beta\sqrt{\Omega}}{2}\left(1-\cosh\frac{\sqrt{\Omega}}{2}\cos\frac{\sqrt{\Omega}}{2}\right), \tag{56}$$

for symmetric mode and

$$\sinh\frac{\sqrt{\Omega}}{2}\cos\frac{\sqrt{\Omega}}{2}-\cosh\frac{\sqrt{\Omega}}{2}\sin\frac{\sqrt{\Omega}}{2}=0, \tag{57}$$

for antisymmetric mode are recovered from (52) and (53), respectively.

2.3.2. Approximate fundamental frequency

To obtain an explicit expression for the fundamental frequency for this case, making use of (20) and after integrating both sides of (7) with respect to ξ we get Eq. (21). Owing to antisymmetric vibration is not influenced by an attached mass placed at the middle of a clamped beam, in what follows symmetric vibration is only concerned. Solving A and B through the boundary conditions in (49) gives

$$A=\frac{1}{2}\int_0^{1/2}s(1-s)\kappa(s)ds+\frac{\beta}{2}\int_0^{1/2}s\kappa(s)ds, \tag{58}$$

$$B=\frac{1}{12}\int_0^{1/2}(1-s)(2-s+s^2)s\kappa(s)ds-\lambda^2\int_0^{1/2}s(1-s)\kappa(s)ds-\frac{\beta}{16}\int_0^{1/2}s\kappa(s)ds. \tag{59}$$

Next, substitution of the above results (58) and (59) into (21) leads to an integral equation, which is omitted here for saving space. Adopting an analogous procedure and taking into account the requirement $\int_0^{1/2}\kappa(s)ds=0$, we choose $\varphi_j(\xi)=\cos(2j\pi\xi)$. The first-order approximation of the fundamental frequency is obtained to be

$$\Omega_1=\frac{4\pi^2}{\sqrt{3+8\beta+4\pi^2\lambda^2}}. \tag{60}$$

As a check, consider a special case of $\beta=\lambda=0$ and we have $\Omega_1=22.79$, which has only a relative error 1.9% as compared to the corresponding classical fundamental frequency $\Omega_1=22.373$. In the presence of β and λ, such an explicit expression for calculating the fundamental frequency seems not to be reported, to the best of the authors' knowledge. In addition, if the fundamental frequency is only focused, we also select $\varphi(\xi)=1-4\xi$ and get an alternative first-order approximation expression for the fundamental frequency, i.e.

$$\Omega_1=\frac{8}{\sqrt{\frac{13}{105}+\frac{1}{3}\beta+\frac{8}{5}\lambda^2}}. \tag{61}$$

The above approximation also gives extremely accurate fundamental frequency. If the dimensionless nonlocal scale parameter $\lambda=0$, we find that (61) nearly equals to $\Omega_1=13.86\sqrt{(0.375+\beta)}$ ([30], p. 492). Furthermore, in the case of $\beta=\lambda=0$, $\Omega_1=22.736$ follows from (61), only 1.6% less than the exact value $\Omega_1=22.373$.

3. Results and discussion

In this section, illustrative examples are presented to show the effect of an attached mass and the nonlocal parameter on the

Table 1
First three dimensionless frequencies Ω_n with $e_0a/L = 0.1$.

End condition	Mode number	β						
		0	0.2	0.5	1	2	5	10
CF	1st	3.5313	2.6203	2.0200	1.5591	1.1590	0.7572	0.5415
	2nd	20.6796	17.2009	15.9842	15.3759	15.0124	14.7711	14.6863
	3rd	51.0638	44.7911	43.2472	42.5739	42.1988	41.9600	41.8780
SS	1st	9.4159	8.0577	6.8013	5.5895	4.3512	2.9450	2.1346
	2nd	64.6414	60.04244	56.9767	54.8081	53.2002	51.9631	51.4908
	3rd	132.5067	127.9126	125.3756	123.7908	122.7132	121.9352	121.6490
CC	1st	21.1090	17.4977	14.4108	11.6170	8.9048	5.9517	4.2926
	2nd	85.7164	81.0824	78.2256	76.3146	74.9549	73.9411	73.5614
	3rd	156.7404	152.0319	149.5328	148.0051	146.9800	146.2462	145.9776

Remark: Only resonance frequencies of symmetric vibration mode are calculated for SS and CC sensors with a mass at the middle, CF: clamped-free; SS: simply-supported; CC: clamped–clamped.

Table 2
First three dimensionless frequencies Ω_n with $\beta = 0.5$.

End condition	Mode number	e_0a/L					
		0	0.02	0.05	0.1	0.15	0.2
CF	1st	2.0163	2.0164	2.0172	2.0200	2.0248	2.0315
	2nd	16.9014	16.8619	16.6587	15.9842	15.0095	13.8822
	3rd	51.7009	51.2631	49.1332	43.2472	36.8872	31.4154
SS	1st	6.9660	6.9592	6.9237	6.8013	6.6110	6.3694
	2nd	71.8155	70.9873	67.0606	56.9767	47.0811	39.1794
	3rd	212.0422	204.5639	175.1513	125.3756	93.2215	73.1648
CC	1st	14.8000	14.7838	14.6998	14.4108	13.9643	13.4030
	2nd	99.9981	98.7613	92.9332	78.2256	64.1245	53.0693
	3rd	259.2049	249.4732	211.7076	149.5328	110.4258	86.4214

Remark: Only resonance frequencies of symmetric vibration mode are calculated for SS and CC sensors with a mass at the middle, CF: clamped-free; SS: simply-supported; CC: clamped–clamped.

Table 3
Locations of nodes (x) and corresponding phase velocities (v) of a vibrating cantilever nanosensor carrying a mass with $\beta = 0.5$.

e_0a/L	Mode 1		Mode 2			Mode 3			
	v/v_1	x/L	v/v_1	x/L		v/v_1	x/L		
0	1	0	2.895	0	0.923	5.064	0	0.549	0.969
0.2	1.004	0	2.624	0	0.929	3.947	0	0.570	0.968
0.4	1.016	0	2.183	0	0.956	3.055	0	0.587	0.951

Table 4
Locations of nodes (x) and corresponding phase velocities (v) of a vibrating cantilever nanosensor carrying a mass with $e_0a/L = 0.2$.

β	Mode 1		Mode 2			Mode 3			
	v/v_1	x/L	v/v_1	x/L		v/v_1	x/L		
0	1	0	2.216	0	0.790	3.207	0	0.512	0.850
0.5	0.753	0	1.969	0	0.929	2.963	0	0.570	0.968
1	0.661	0	1.934	0	0.958	2.939	0	0.576	0.982
2	0.570	0	1.912	0	0.976	2.926	0	0.579	0.991

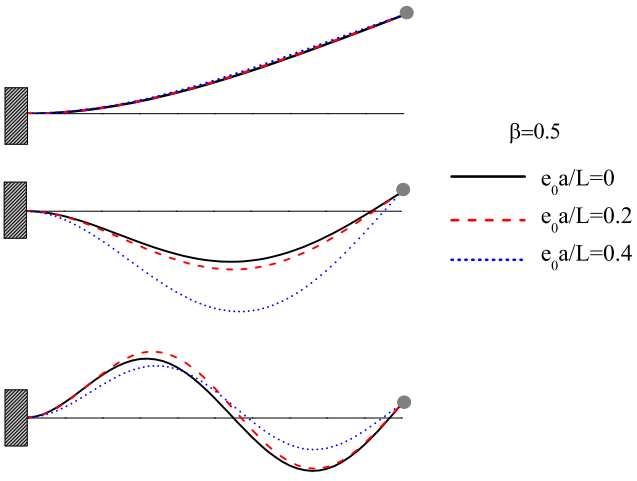

Fig. 2. Mode shapes of a cantilever nanosensor carrying a mass with $\beta = 0.5$.

resonance frequencies, in particular on the fundamental frequencies. Furthermore, mass identification of sensors is analyzed.

3.1. Resonance frequencies

In the foregoing section, we have derived the frequency equation for each case. With these frequency equations, the resonance frequencies can be determined by solving these transcendental equations. To show the dependence of the resonance frequencies on an attached mass and the nonlocal parameter, we calculate resonance frequencies and list them in Tables 1 and 2 for $e_0a/L = 0.1$ and $\beta = 0.5$, respectively. From Table 1, one finds that due to addition of attached mass, the vibration frequencies decline, as expected. On the other hand, for a given mass, the effect of nonlocal parameter on the resonance frequency is also viewed in Table 2. For simply-supported and clamped–clamped nonlocal beams carrying a mass, the influence of the nonlocal parameter decreases the resonance frequencies. Moreover, with the order of vibration mode rising, the influence becomes stronger. This also implies that for a shorter sensor, the nonlocal effect leads to a decrease of the resonance frequencies since e_0a/L is raised.

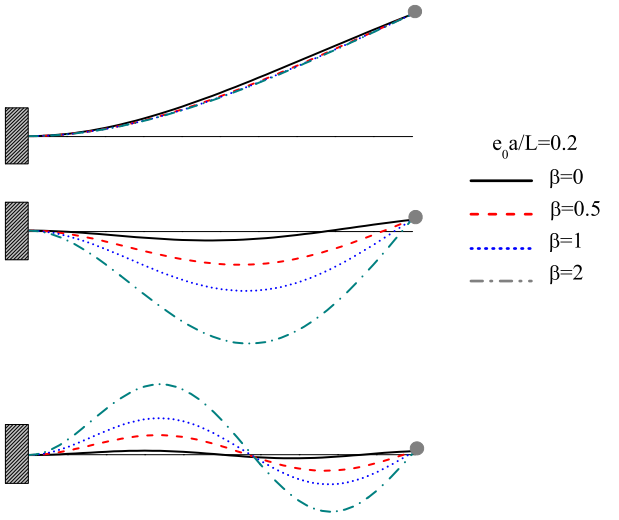

Fig. 3. Mode shapes of a cantilever nanosensor carrying a mass with $e_0a/L = 0.2$.

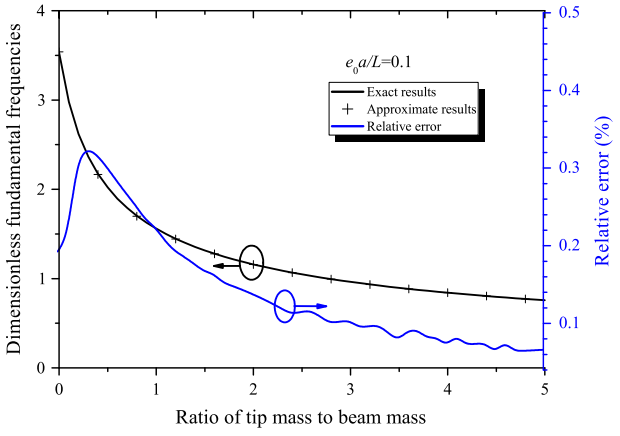

Fig. 4. Comparison of fundamental frequencies for clamped-free cantilever sensors via solving the frequency equation and using first-order approximation.

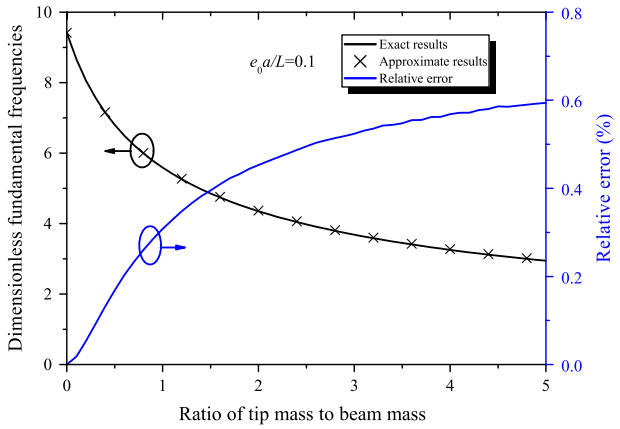

Fig. 5. Comparison of fundamental frequencies for simply-supported sensors via solving the frequency equation and using first-order approximation.

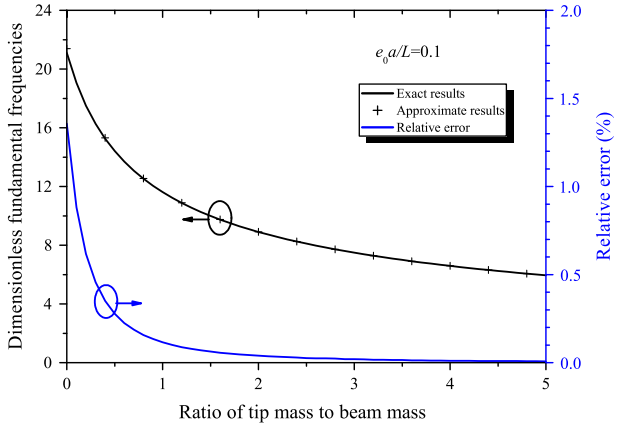

Fig. 6. Comparison of fundamental frequencies for clamped–clamped sensors via solving the frequency equation and using first-order approximation.

However, it is interesting to note that the fundamental frequencies of a cantilevered sensor have an opposite trend to the above observation. In other words, with e_0a/L rising the fundamental frequencies of nanocantilevers increase, while higher-order frequencies decrease.

Another interesting analysis is the variation of the phase velocities on the attached mass and the nonlocal parameter. For a cantilever nanosensor, we list the locations of nodes and corresponding phase velocities for the fundamental and overtone frequencies with $\beta = 0.5$ in Table 3, where $v_1 = \sqrt{\omega_1 c r_g}$. Similarly, for a given nonlocal parameter $e_0a/L = 0.2$, the locations of nodes and corresponding phase velocities for the fundamental and overtone frequencies for several mass ratios are tabulated in Table 4. In contrast, we also plot the first three mode shapes of a cantilever nanosensor for two different cases in Figs. 2 and 3.

3.2. Verification of approximate frequencies

Although the equations for determining the resonance frequencies have been derived for cases of interest, they are all transcendental equations, whose roots can be determined by numerically solving these equations. It is unlikely that a dependence of the resonance frequencies on an attached mass and the nonlocal parameter can be given in explicit form. However, giving an explicit dependence of the resonance frequencies on the nonlocal parameter and the attached mass parameter is beneficial to identification of the magnitude of an attached mass. Due to this reason, in the above we have employed the integral equation method to obtain respective explicit expression for the fundamental frequency for each case. Here we give a comparison of the results based on the above-derived approximations and their corresponding exact frequency equations.

Figs. 4–6 give a comparison of the dimensionless fundamental frequencies against the ratio β of the attached mass to the beam mass for $e_0a/L = 0.1$ by solving the corresponding transcendental equations and using the first-order approximations for cantilevered, simply-supported and bridged sensors, respectively. Here we select (29), (47) and (61) as their first-order approximations, respectively. From Figs. 4–6 it is viewed that the relative error does not exceed 0.4%, 0.6%, and 1.4%, respectively, for cantilevered, simply-supported, and bridged sensors carrying a nanoparticle with mass lighter than five times as much as the beam mass. Although the maximum error for clamped sensors reaches 1.4%, which occurs in the case of no attached mass, the relative error immediately decreases to 0.88% only for the attached mass exceeding 10 percent of the mass of a nanobeam. Therefore, we can say that these first-order approximations provide a satisfactory estimation of the fundamental frequencies with accuracy of 99.6%, 99.4% and 98.6%, respectively.

Table 5
Comparison of the frequency parameter $\sqrt{\Omega_1}$ with $\beta = 0$ for a nanocantilever.

e_0a/L	$\beta = 0$			$\beta = 0.5$		
	Exact [28]	(29) [Present]	(30) [24]	Exact [Present]	(29) [Present]	(30) [24]
0	1.8751	1.8752	1.8888	1.4200	1.4177	1.4210
0.1	1.8792	1.8810	1.8655	1.4213	1.4191	1.4153
0.2	1.8919	1.8991	1.8033	1.4253	1.4235	1.3988
0.3	1.9154	1.9313	1.7188	1.4323	1.4309	1.3732
0.4	1.9543	1.9814	1.6274	1.4427	1.4416	1.3410
0.5	2.0219	2.0567	1.5383	1.4574	1.4559	1.3046
0.6	2.1989	2.1726	1.4559	1.4778	1.4745	1.2660

Table 6
Comparison of the calibration constants.

	Cantilevered			Bridged			Simply-supported
	Present	[24]	[12]	Present	[10]	[12]	Present
c_k	3.516	3.568	3.516	22.373	22.736	22.373	9.870
c_m	4.121	4.242	4	2.692	2.692	2.522	2
c_n	−1.236	5.091	–	12.923	–	–	9.870

As mentioned before, our first-order approximation (29) for nanocantilever sensors is different from the one derived in [24], i.e. (30). Here we examine their accuracy by comparing numerical results of the frequency parameter $\sqrt{\Omega_1}$ with the exact ones by solving the frequency Eq. (15) in Table 5. Notice that the exact results in the case of $\beta = 0$ can be found in [28]. From (29) and (30), it is observed that a main difference results from the term related to the nonlocal parameter, which gives an opposite trend to affect the frequency. From Table 5, one finds that for a large range of e_0a/L, our results are closer to the exact ones than those in [24], which infers that our expression (29) for the fundamental frequency provides a more accurate approximation.

3.3. Mass identification

Owing to the exact resonance frequencies being transcendental equations, it is nearly unlikely to gain an explicit relation between the resonance frequency and the attached mass. Instead, it can be achieved by the first-order approximations of the resonance frequencies derived above. To do this, it is found that a unified expression for the dimensionless fundamental frequency Ω can be written as

$$\frac{1}{\Omega} = \frac{1}{c_k}\sqrt{1 + c_m\beta + c_n\lambda^2}, \tag{62}$$

where c_k, c_m and c_n are calibration constants, which are tabulated in Table 6. Here c_k corresponds to the dimensionless fundamental frequency without any attached mass and any the nonlocal effect, i.e. $\beta = \lambda = 0$.

After algebra one obtains

$$\frac{\Delta f_c}{f}\left(\frac{\Delta f_c}{f} + 2\right) = c_m\beta + c_n\lambda^2, \tag{63}$$

where f denotes the fundamental frequency, and Δf_c is the frequency shift, i.e. $\Delta f_c = f_{0c} - f$, f_{0c} being the classical fundamental frequency corresponding to $\beta = \lambda = 0$. From the above, the mass of an attached nanoparticle can be expressed below

$$\frac{m}{m_b} = \frac{\Delta f_c}{c_m(f_{0c} - \Delta f_c)}\left(\frac{\Delta f_c}{f_{0c} - \Delta f_c} + 2\right) - \frac{c_n}{c_m}\lambda^2, \tag{64}$$

where m_b stands for the mass of sensor (beam). Furthermore, considering the fact that the frequency shift is low as compared with the fundamental frequency, one can approximate the above result as

$$\frac{m}{m_b} = \frac{\Delta f_c}{c_m f_{0c}}\left[2 + 3\frac{\Delta f_c}{f_{0c}} + 4\left(\frac{\Delta f_c}{f_{0c}}\right)^2\right] - \frac{c_n}{c_m}\lambda^2. \tag{65}$$

It is seen that the size effect reflected by the nonlocal parameter has a contribution on mass identification. If neglecting the nonlocal effect, the mass identification formula

$$\frac{m}{m_b} = \frac{2\Delta f_c}{c_m f_{0c}}, \tag{66}$$

is recovered [10].

Although the above result provides a method for identifying attached mass, it is still inconvenient to use since the above result is based on the frequency shift $\Delta f_c = f_{0c} - f$ relative to the classical fundamental frequency f_{0c}. In fact, for a biosensor in the order of nanometer, the classical fundamental frequency f_{0c} is nearly of

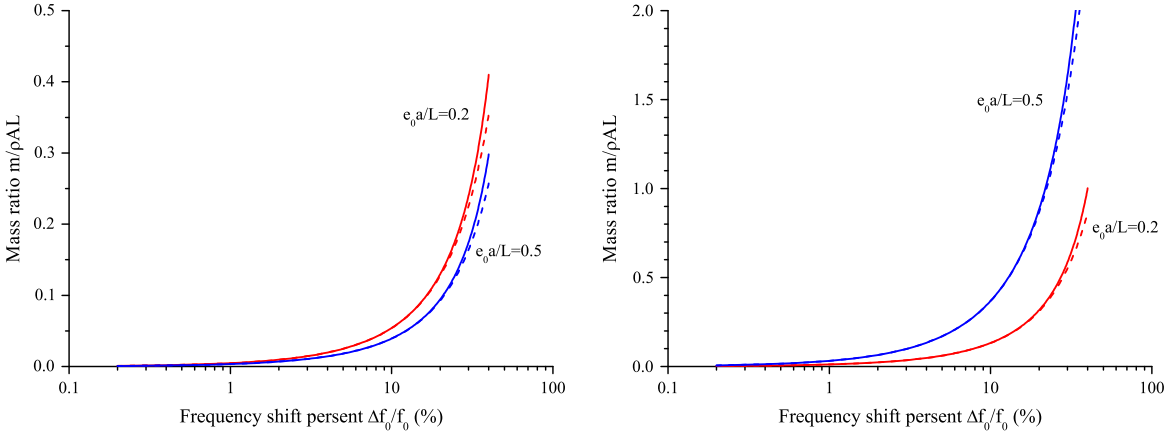

Fig. 7. A comparison of the exact mass identification (68) and its approximation (69) for cantilevered and bridged nanosensors with $e_0a/L = 0.2,\ 0.5$, where the solid lines represent the predictions using (68) and dashed lines represent those using (69), (a) for a cantilevered nanosensor; (b) for a bridged nanosensor.

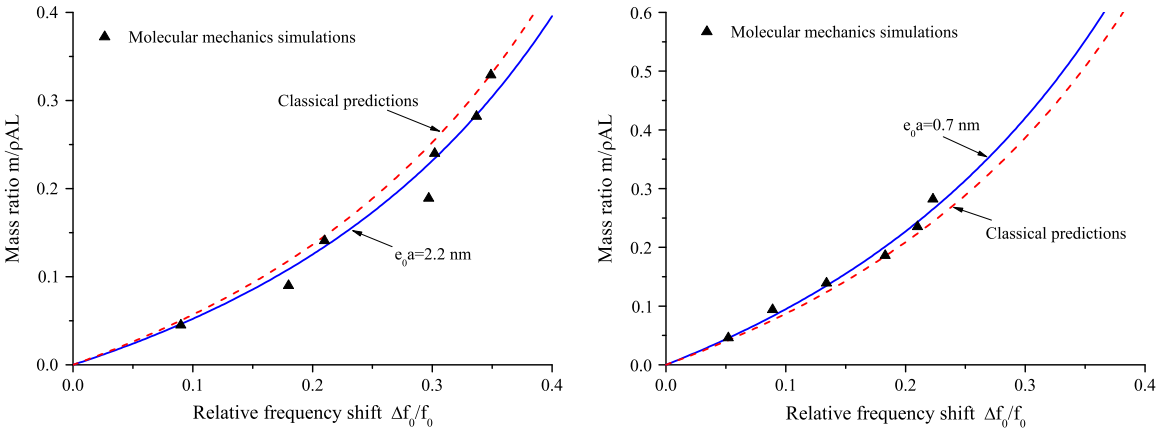

Fig. 8. Predicted values of attached mass based on the mass identification (68) from the frequency shift, where scattered data are taken from [12], which were evaluated via the molecular mechanics approach, (a) for a cantilevered nanosensor; (b) for a bridged nanosensor.

no use since the measured frequencies exhibit the size effects. More useful is the fundamental frequency with $\beta = 0$ and $\lambda \neq 0$. In other words, we only require compare a change in the frequencies before and after a mass is carried. Then for a nanosensor with radius of gyration of the cross-section in nanometer order, the fundamental frequency without any attached mass is no longer equal to the corresponding classical one thanks to the contribution of the scale effect. As a result, a way to identify mass is more feasible through comparing the frequencies before and after a mass is attached. Denoting f_0 as the fundamental frequency for the free vibration of a nanosensor without any attached mass, we have

$$\frac{1}{f_0} = \frac{1}{f_{0c}}\sqrt{1 + c_n\lambda^2}. \tag{67}$$

Using (67), one gains an alternative expression for mass identification

$$\frac{m}{m_b} = \frac{\Delta f_0}{c_m(f_0 - \Delta f_0)}\left(\frac{\Delta f_0}{f_0 - \Delta f_0} + 2\right)(1 + c_n\lambda^2), \tag{68}$$

where $\Delta f_0 = f_0 - f$ represents a change in the fundamental frequency due to addition of an attached mass. This result indicates that the mass ratio is independent of the equivalent spring coefficient c_k, but depends upon the calibration constants c_m and c_n. In particular, we can give an approximation of the above mass identification (68), i.e.

$$\frac{m}{m_b} = \frac{(1 + c_n\lambda^2)\Delta f_0}{c_m f_0}\left[2 + 3\frac{\Delta f_0}{f_0} + 4\left(\frac{\Delta f_0}{f_0}\right)^2\right]. \tag{69}$$

The approximation (69) is extremely effective for the frequency shift percent less than 20%, and the error of predicted mass ratio does not exceed 2%. When the frequency shift is larger than 30%, the predicted mass gradually deviates away from the exact one in excess of 6% and in this case the exact mass identification (68) is required. If ignoring the scaling factor, (69) collapses to (66), as expected. Fig. 7 shows a comparison of the exact mass identification (68) and its approximation (69) for cantilevered and bridged nanosensors, where the nonlocal parameter is chosen as $e_0a/L = 0.2, 0.5$. By comparing (69) with the classical one, corresponding to $\lambda = 0$, we find that the contribution of the scaling factor is different. The nonlocal parameter decreases the predicted mass for cantilever sensors, but increases it for bridged sensors. Or rather, the predicted mass is overestimated for cantilever sensors, and underestimated for bridged sensors, if the classical mass identification formula is used.

The approximation (69) provides a scheme to identify the mass of an attached nanoparticle. A rough estimation allows us to judge that a CNT cantilever with weight of about 10^{-24} kg can be used as a sensor to detect a mass with atomic resolution. This can be used to interpret basic principle of zeptogram-scale nanosensors. In fact, some experiments have confirmed that mass resolution achieved by CNT resonators can reach as low as 10^{-24} kg [4,5,32].

As an illustrative example, we consider a zigzag $(5, 0)$ single-walled CNT oscillator of length 8.52 nm as a biosensor, which can be used to detect a zeptogram-scale mass. Here we choose deoxythymidine, a nucleotide found in DNA, as an added concentrated mass. The frequency shifts have been calculated via the molecular mechanics approach [12], which from a microscopic viewpoint assumes that the general expression of total energy is a sum of energies due to bonded interactions (consisting of bond stretching and angular distortions) and nonbonded interactions (including van der Waals and/or electrostatic terms) [33,34]. These data are used to examine the efficiency of the present method. Using the above mass identification formula (68), we plot predicted mass and the corresponding molecular mechanics simulations in Fig. 8(a) and (b) for cantilevered biosensor and bridged biosensor, respectively. If neglecting the contribution of the scaling factor ($c_n = 0$), we find that as compared with the attached mass used in molecular mechanics simulations, the predicted values of attached mass are somewhat overestimated for a cantilevered CNT-based biosensor, and slightly underestimated for a bridged CNT-based biosensor, respectively. Although these errors are miniscule, by careful inspection, one observes that predicted masses are all above the molecular mechanics simulations for cantilevered biosensor, and all below the molecular mechanics simulations for bridged biosensor. This suggests that although the classical theory is capable of predicting a rough trend of attached mass against the frequency shift, it has a systematic error, rather than random error. The cause is due to lack of the scale factor in the classical beam theory, and it is therefore not quite adequate and cannot completely capture the accurate dependence of the attached mass upon the frequency shift because a systematic error between the predicted masses and the obtained data from the molecular mechanics approach is clearly viewed. Consequently, if considering the effect of the scaling factor, it is seen that the accuracy of the predicted values of attached mass is improved and the systematic error between the predicted masses and the molecular mechanics simulations is eliminated save random error. The estimated mass values are closer to those in the molecular mechanics simulations, regardless of a cantilevered CNT-based biosensor or a bridged CNT-based biosensor. Finally, it is worth noting that the above formulation

only suits for slender biosensors, and is not applicable to short biosensors because the present approach is based on the simplest beam theory, i.e. nonlocal Euler–Bernoulli theory of beams, which neglects shear deformation and rotary inertia of the cross section. For predominant wavelengths around the order of the radius of gyration of the nanosensors, the equation of motion of flexural waves should be employed according to the nonlocal Timoshenko beam model [35].

4. Conclusions

This paper studied flexural vibration of CNT beams as zeptogram-scale nanosensors carrying a concentrated nanoparticle. The nonlocal Euler–Bernoulli beam theory has been used and the nonlocal effect was applied to describe the size effect of the mechanical properties of CNTs. The frequency equations were derived and resonance frequencies were calculated. In addition, the integral equation method was employed to obtain approximate fundamental frequencies in explicit form. Obtained results are drawn as follows.

- Explicit expressions for the fundamental frequencies are obtained.
- Addition of attached mass decreases the natural frequencies of a mass-beam resonator.
- The nonlocal parameter deceases the frequencies except for the fundamental frequency of cantilever sensors.
- Mass identification formulae of nanoscale sensors including the size effects are provided.

Acknowledgements

This work was supported by the Open Foundation of State Key Laboratory of Structural Analysis for Industrial Equipment, Dalian University of Technology, P.R. China (No. GZ1308), the Faculty Research Foundation of Central South University, P.R. China (No. 2013JSJJ020), and the National Natural Science Foundation of China (No. 11302254). The useful suggestions from an Associate Editor Prof. P.A. Lewin for the improvement of the quality of the original manuscript were very much appreciated.

References

[1] J.L. Arlett, E.B. Myers, M.L. Roukes, Comparative advantages of mechanical biosensors, Nature Nanotechnol. 6 (2011) 203–215.
[2] J.H. Hafner, C.L. Cheung, A.T. Woolley, C.M. Lieber, Structural and functional imaging with carbon nanotube AFM probes, Prog. Biophys. Mol. Biol. 77 (2001) 73–110.
[3] D. Garcia-Sanchez, A. San Paulo, M.J. Esplandiu, F. Perez-Murano, L. Forro, A. Aguasca, A. Bachtold, Mechanical detection of carbon nanotube resonator vibrations, Phys. Rev. Lett. 99 (2007) 85501.
[4] K. Jensen, K. Kim, A. Zettl, An atomic-resolution nanomechanical mass sensor, Nature Nanotechnol. 3 (2008) 533–537.
[5] B. Lassagne, D. Garcia-Sanchez, A. Aguasca, A. Bachtold, Ultrasensitive mass sensing with a nanotube electromechanical resonator, Nano Lett. 8 (2008) 3735–3738.
[6] X.L. Feng, R.R. He, P.D. Yang, M.L. Roukes, Very high frequency silicon nanowire electromechanical resonators, Nano Lett. 7 (2007) 1953–1959.
[7] E. Gil-Santos, D. Ramos, J. Martinez, M. Fernindez-Regulez, R. Garcia, A. San Paulo, M. Calleja, J. Tamayo, Nanomechanical mass sensing and stiffness spectrometry based on two-dimensional vibrations of resonant nanowires, Nature Nanotechnol. 5 (2010) 641–645.
[8] C.Y. Li, T.W. Chou, Single-walled carbon nanotubes as ultrahigh frequency nanomechanical resonators, Phys. Rev. B 68 (2003) 073405.
[9] C.Y. Li, T.W. Chou, Mass detection using carbon nanotube-based nanomechanical resonators, Appl. Phys. Lett. 84 (2004) 5246–5248.
[10] R. Chowdhury, S. Adhikari, J. Mitchell, Vibrating carbon nanotube based biosensors, Physica E 42 (2009) 104–109.
[11] A.Y. Joshi, S.P. Harsha, S.C. Sharma, Vibration signature analysis of single walled carbon nanotube based nanomechanical sensors, Physica E 42 (2010) 2115–2123.
[12] S. Adhikari, R. Chowdhury, The calibration of carbon nanotube based bionanosensors, J. Appl. Phys. 107 (2010) 124322.
[13] P. Poncharal, Z.L. Wang, D. Ugarte, W.A. de Heer, Electrostatic deflections and electromechanical resonances of carbon nanotubes, Science 283 (1999) 1513–1516.
[14] C.Q. Chen, Y. Shi, Y.S. Zhang, J. Zhu, Y.J. Yan, Size dependence of Young's modulus in ZnO nanowires, Phys. Rev. Lett. 96 (2006) 75505.
[15] X.-F. Li, H. Zhang, K.Y. Lee, Dependence of Young's modulus of nanowires on surface effect, Int. J. Mech. Sci. 81 (2014) 120–125.
[16] X.X. Li, T. Ono, Y.L. Wang, M. Esashi, Ultrathin single-crystalline-silicon cantilever resonators: fabrication technology and significant specimen size effect on Young's modulus, Appl. Phys. Lett. 83 (2003) 3081–3083.
[17] T. Murmu, S. Adhikari, Nonlocal vibration of carbon nanotubes with attached buckyballs at tip, Mech. Res. Commun. 38 (2011) 62–67.
[18] T. Murmu, S. Adhikari, Nonlocal frequency analysis of nanoscale biosensors, Sens. Actuat. A: Phys. 173 (2012) 41–48.
[19] Z.B. Shen, X.F. Li, L.P. Sheng, G.J. Tang, Transverse vibration of nanotube-based micro-mass sensor via nonlocal Timoshenko beam theory, Comput. Mater. Sci. 53 (2012) 340–346.
[20] Z.B. Shen, G.J. Tang, L. Zhang, X.F. Li, Vibration of double-walled carbon nanotube based nanomechanical sensor with initial axial stress, Comput. Mater. Sci. 58 (2012) 51–58.
[21] Z.B. Shen, L.P. Sheng, X.F. Li, G.J. Tang, Nonlocal Timoshenko beam theory for vibration of carbon nanotube-based biosensor, Physica E 44 (2012) 1169–1175.
[22] T. Natsuki, N. Matsuyama, J.-X. Shi, Q.-Q. Ni, Vibration analysis of nanomechanical mass sensor using carbon nanotubes under axial tensile loads, Appl. Phys. A (2014) 1–7.
[23] S. Souayeh, N. Kacem, Computational models for large amplitude nonlinear vibrations of electrostatically actuated carbon nanotube-based mass sensors, Sens. Actuat. A: Phys. 208 (2014) 10–20.
[24] T. Murmu, S. Adhikari, Nonlocal frequency analysis of nanoscale biosensors, Sens. Actuat. A: Phys. 173 (2012) 41–48.
[25] I. Elishakoff, N. Challamel, C. Soret, Y. Bekel, T. Gomez, Virus sensor based on single-walled carbon nanotube: improved theory incorporating surface effects, Philos. Trans. Roy. Soc. A: Math. Phys. Eng. Sci. 371 (2013) 20120424.
[26] A.C. Eringen, On differential equations of nonlocal elasticity and solutions of screw dislocation and surface waves, J. Appl. Phys. 54 (1983) 4703–4710.
[27] J.N. Reddy, Nonlocal theories for bending, buckling and vibration of beams, Int. J. Eng. Sci. 45 (2007) 288–307.
[28] P. Lu, H.P. Lee, C. Lu, P.Q. Zhang, Dynamic properties of flexural beams using a nonlocal elasticity model, J. Appl. Phys. 99 (2006) 073510.
[29] Y. Huang, X.-F. Li, A new approach for free vibration of axially functionally graded beams with non-uniform cross-section, J. Sound Vib. 329 (2010) 2291–2303.
[30] W.D. Pilkey, W.D. Pilkey, W.D. Pilkey, Formulas for Stress, Strain, and Structural Matrices, John Wiley & Sons, New Jersey, 2005.
[31] I.A. Karnovsky, O.I. Lebed, Formulas for Structural Dynamics: Tables, Graphs and Solutions, McGraw-Hill, New York, 2004.
[32] Y.T. Yang, C. Callegari, X.L. Feng, K.L. Ekinci, M.L. Roukes, Zeptogram-scale nanomechanical mass sensing, Nano Lett. 6 (2006) 583–586.
[33] A.K. Rappe, C.J. Casewit, K. Colwell, W. Goddard Iii, W. Skiff, UFF, a full periodic table force field for molecular mechanics and molecular dynamics simulations, J. Am. Chem. Soc. 114 (1992) 10024–10035.
[34] C.Y. Li, T.-W. Chou, A structural mechanics approach for the analysis of carbon nanotubes, Int. J. Solids Struct. 40 (2003) 2487–2499.
[35] X.-F. Li, B.-L. Wang, Vibrational modes of Timoshenko beams at small scales, Appl. Phys. Lett. 94 (2009) 101903.